3-Dimensional Numerical Calculations Considering Geotechnical Measurement Data

Christian Volderauer, Thomas Marcher & Robert Galler

Springer

Springer

BHM Berg- und Hüttenmännische Monatshefte

3-Dimensional Numerical Calculations Considering Geotechnical Measurement Data

Christian Volderauer[1], Thomas Marcher[1] and Robert Galler[2]

[1]ILF Consulting Engineers ZT GmbH, Rum, Austria
[2]Chair of Subsurface Engineering, Montanuniversitaet Leoben, Austria

Abstract: This paper discusses the numerical analysis of a specific part of the deep seated Gotthard Base Tunnel. A section of the western tube situated in the Clavaniev Zone was simulated with the finite element programme ABAQUS. Geological and geotechnical documentation from the design stage and the construction stage as well as daily and monthly reports of the construction site were provided by AlpTransit Gotthard Ltd. This documentation has been used to perform 3-dimensional analyses with implementation of support elements in a realistic construction sequence. For the simulations different constitutive laws were used. The aim of this research project was to investigate whether measurements of radial deformations and the core extrusion in front of the face can be matched with the results of 3-dimensional FE simulations based on information available during the design and the construction stage.

Keywords: Gotthard Base Tunnel, 3-dimensional numerical simulation, Depth-dependent Young's modulus

3-dimensionale numerische Simulationen unter Berücksichtigung von geotechnischen Messergebnissen

Zusammenfassung: In diesem Paper werden die Ergebnisse 3-dimensionaler numerischer Simulationen eines Abschnitts der Weströhre in der geologischen Formation der Clavaniev Zone des tiefliegenden Gotthard Basistunnels angeführt. Die geologische und geotechnische Dokumentation aus der Planungs- und der Ausführungsphase sowie die Tages- und Monatsberichte wurden von der AlpTransit Gotthard Ltd zur Verfügung gestellt. Auf Basis dieser Dokumentation wurden 3-dimensionale Simulationen unter Verwendung verschiedener Materialmodelle durchgeführt. In diesem Forschungsprojekt wurde untersucht, ob die Messergebnisse der radialen Verformungen sowie der axialen Verformungen vor der Ortsbrust mit den Ergebnissen der 3-dimensionalen Simulationen übereinstimmen.
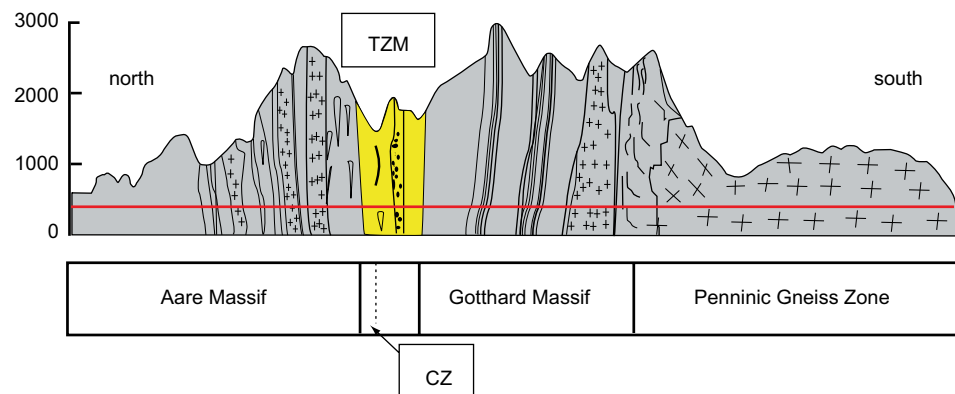
Schlüsselwörter: Gotthard Basistunnel, 3-dimensionale numerische Simulation, Tiefenabhängiger Elastizitätsmodul

1. Introduction

Major tunnelling projects with very high overburdens were built in Switzerland within the last decades. One famous example is the Gotthard Base Tunnel, the longest railway tunnel in the world. For a research project including the Chair of Subsurface Engineering, Montanuniversitaet Leoben and ILF Consulting Engineers ZT GmbH, geological and geotechnical documentation from the design and the construction stage as well as daily and monthly reports of the construction site and results from measurements were provided by AlpTransit Gotthard Ltd for a specific part of the Gotthard Base Tunnel. AlpTransit Gotthard Ltd is the constructor of the Gotthard axis of the New Rail Link through the Alps with base tunnels through the Gotthard and Ceneri. The aim of this research project was to investigate whether the measurement results from the construction site can be matched with the results of 3-dimensional FE simulations based on information available during the design and the construction stage.

Dipl.-Ing. C. Volderauer (✉)
ILF Consulting Engineers ZT GmbH, Feldkreuzstraße 3,
6063 Rum, Austria
e-mail: Christian.Volderauer@ilf.com

Fig. 1: Schematic geological section of the Gotthard Base Tunnel (according to Kovari [1])

2. Gotthard Base Tunnel

2.1 Geological and Geotechnical Parameters for the Investigated Section

For the actual research project a 35 m long section of the western tube of the new Gotthard Base Tunnel situated in the Clavaniev Zone (CZ) between the northern intermediate Tavetsch formation (TZM) and the Aare Massif was investigated. The section of interest is at the end of the Clavaniev Zone at the transition to the Aare Massif (Fig. 1), starts at chainage 2090 and ends at chainage 2125. This section was chosen based on the available documentation of:

- monitoring of stratification and cleavage;
- measuring data of deformations in the tube due to an intensive monitoring programme;
- geotechnical parameters, gathered during design and construction stage;
- excavation and support measures;
- measuring data of the installed reverse-head extensometers (RH extensometers).

The Clavaniev Zone and the intermediate Tavetsch formation consist of gneisses, slates and phyllites in layers of decimetres to decametres. The quality of these rock masses varies from intact to more or less kakiritic.

A laboratory testing programme in the design stage was performed to investigate the strength and deformation properties of specimens retrieved from a 1,700 m long exploratory borehole [2]. By means of this borehole the expected squeezing conditions in the intermediate Tavetsch formation and the Clavaniev Zone were investigated. During the construction stage laboratory tests were performed on specimens retrieved from boreholes from the tunnel face [3].

2.2 Construction Method

Full face excavation of the tunnel was carried out using tunnel excavators with lengths of rounds of 1.34 m to 1.0 m. The excavation radius was between 5.89 and 6.24 m with an over-excavation of 0.5 and 0.7 m to accommodate the predicted deformations. To handle these deformations, two overlapping rings of sliding steel arches (TH 44/70) were installed as yielding support elements after each round, with a spacing of 0.66 or 0.5 m. After convergences subsided, these two rings were rigidly connected by closing friction loops. Furthermore, up to 26 rock bolts, each with a length of 8 m, were installed over the whole circumference of the tunnel after each round. About 30 m behind the face a shotcrete lining of 0.5 m was applied. To provide a safe face, 50 to 60 pieces of 12–18 m long IBO-bolts with an overlap of 6–9 m and a 0.1 m thick shotcrete lining were installed.

2.3 Measurement Programme

Optical measurements were performed with 5–7 points per cross section in a distance between measuring sections from 4 m to 13 m. RH-Extensometers [4], a new development in the field of geotechnical monitoring for determining the pre-displacements in front of the face, were installed in the Gotthard Base Tunnel for the very first time. The core extrusion was measured with seven pieces of 24 m long RH-Extensometers at the axis of the tunnel. Each set of RH-Extensometers overlapped 4–8 m with the preceding ones to provide a continuous measurement of the core extrusion. The results from the measurement of the core extrusion are shown in Fig. 2.

The magnitude of the measured deformations in front of the face is about 400 mm for three RH-Extensometers. The others are significantly smaller and vary from 10 to 230 mm. The difference in this dimension most likely results from changing geological/geotechnical conditions.

3. Finite Element Model

3.1 Model Design

For 3-dimensional numerical simulations a model was generated with a size of 100 m in depth, 200 m in height and 118 m in length, with a total of 135,000 hexagonal linear elements using the software ABAQUS. The overburden of the selected area is about 960 m, by choosing a specific weight of 25 kN/m^3 a primary stress level of 24 MPa was
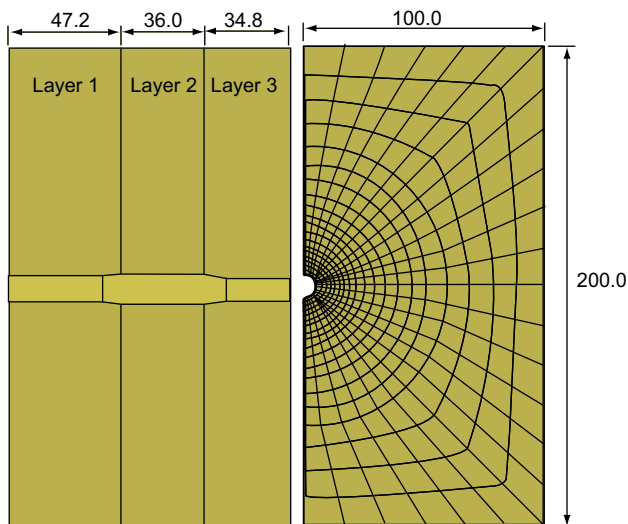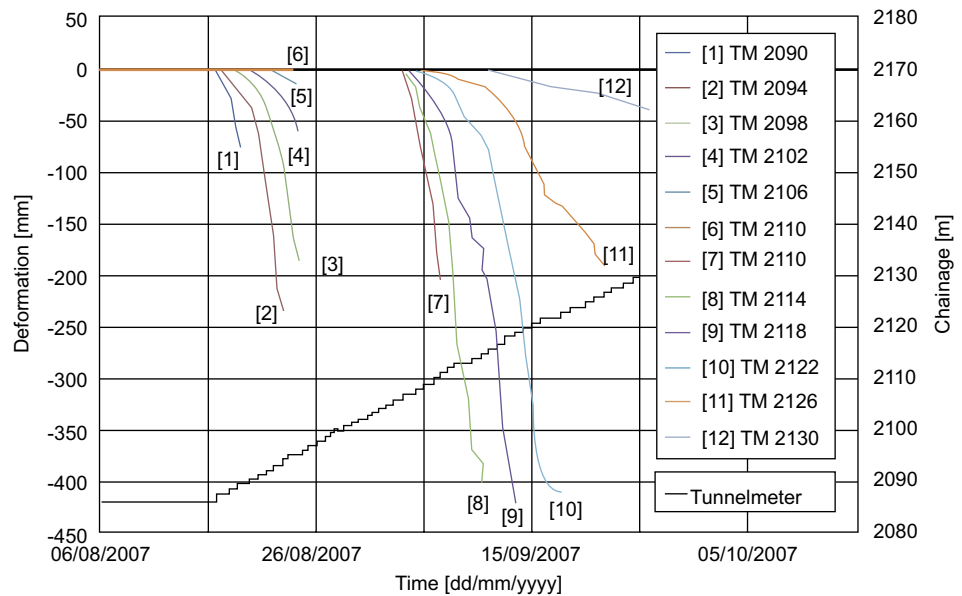
Fig. 2: Measurement results from RH-Extensometers

Fig. 3: **a** Front view of the model including dimensions. **b** Side view of the model including dimensions and mesh

calculated. For numerical simulations a side pressure coefficient of $K_0 = 1.0$ was used. At the bottom of the model, vertical and horizontal boundaries were applied, at the sidewalls of the model, movements in horizontal directions were set to zero. The advance was modelled by deactivating elements of the circular tunnel using the "Model Change" function of ABAQUS. In the initial stage all sup-

port elements were deactivated and re-activated again continuously with ongoing advance.

Three ground layers normal to the tunnel axis were implemented in accordance with the geological section (Fig. 3a). The first two layers are part of the Clavaniev Zone, Layer 3 is characterized by the more competent Aare Massif.

At the end of Layer 1, the tunnel was expanded from 5.89 m to a radius of 6.24 m over a length of about 7 m and at the beginning of the Aare Massif reduced again to 5.18 m over a length of about 10 m (Fig. 3a). Figure 3b shows a cross section of the tunnel and the applied mesh.

3.2 Implemented Constitutive Laws

For numerical simulations linear-elastic ideal-plastic constitutive laws were used. First numerical simulations were performed with a Mohr-Coulomb failure criterion, using ground parameters gathered during the design stage. The rock mass parameters, cohesion (c), friction angle (ϕ) and dilatancy (ψ) are given in Table 1.
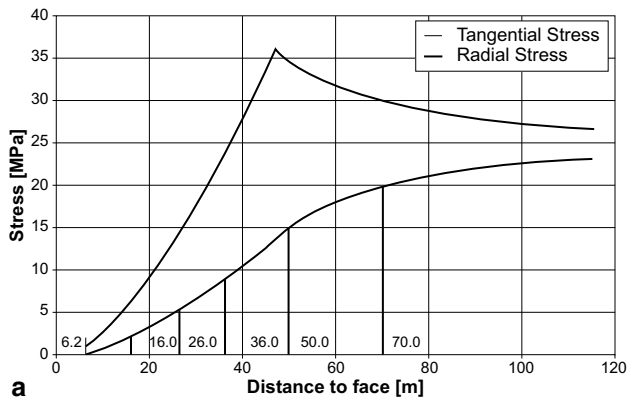
Afterwards a Drucker-Prager failure criterion was used. Models were simulated for the Drucker-Prager criterion with parameters for a compression cone and for an approximation cone to obtain comparable results with the Mohr-Coulomb failure criterion. The parameters, cohesion (d), friction angle (β) and dilatancy (ψ) are shown in Table 2 for the different ground layers for the approximation cone of the Drucker-Prager failure criterion.

TABLE 1: **Ground parameters using a Mohr-Coulomb failure criterion**			
Layer	c (kPa)	ϕ (°)	ψ (°)
1	500	26	5
2	300	26	5
3	1100	29.8	7

TABLE 2: **Ground parameters using a Drucker-Prager failure criterion**			
Layer	d (kPa)	β (°)	ψ (°)
1	740	35.9	8.2
2	445	35.9	8.2
3	1570	29.5	11.4

TABLE 3: Young's moduli in dependence of the depth for the different layers						
Confining Stress Layer	0 (MPa)	2 (MPa)	5 (MPa)	9 (MPa)	15 (MPa)	20 (MPa)
1	1.6	3.0	5.4	7.8	10	10
2	0.8	1.5	2.7	3.9	5.8	7.5
3	4.4	8.3	14.9	21.5	31.9	41.3

Fig. 4: a Determination of the distance to the tunnel perimeter. **b** Distribution of the different Young's moduli in the numerical model

3.3 Use of a Depth-dependent Young's Modulus

Observations show an increase of Young's modulus of rock mass with increasing distance to the tunnel [5]. This depth dependency is even more pronounced in weaker rock masses [6]. As results of first numerical calculations using the initial stiffness properties did not match the measurement data, a depth-dependent Young's modulus was implemented in the numerical model for the different ground sections. Basic data for this approach were results from triaxial tests performed at the Institute of Geotechnical Engineering of the ETH Zurich [3] with lateral pressures of 2, 5 and 9 MPa for Layer 2. With these test results the Young's modulus without side pressure was determined

using the assumptions given in Asef and Reddish [5] and Verman et al. [6] according to Eqs. 1 and 2.

$$E_{\sigma 3(t)} = E_{\sigma 3(t=0)} \frac{200 \frac{\sigma_{3(t)}}{\sigma_{cj}} + b}{\frac{\sigma_{3(t)}}{\sigma_{cj}} + b} \qquad (1)$$

with:

$$b = 15 + 60 e^{-0,18 \, \sigma_{ci}} \qquad (2)$$

Afterwards Young's moduli for side pressures of 15 and 20 MPa (Eq. 1 and Eq. 2) were calculated using Eqs. 1 and 2. Young's moduli for ground layers 1 and 3 were gathered with extrapolation from ground layer 2, based on the original Young's moduli used in the design stage. The calculated Young's moduli and the applied side pressures can be seen in Table 3. As mentioned before, layer 1 and 2 consist of intact and/or kakiritic gneisses, slates and phyllites. The highest value for Young's moduli for these sections was chosen to be the modulus of intact phyllite, which is about 10 GPa.

With these results the distances to the tunnel perimeter for the different Young's moduli were calculated using an analytical approach according to Sulem et al. [7] (Fig. 4a). The implementation in the model and the range of each Young's modulus can be seen in Fig. 4b.
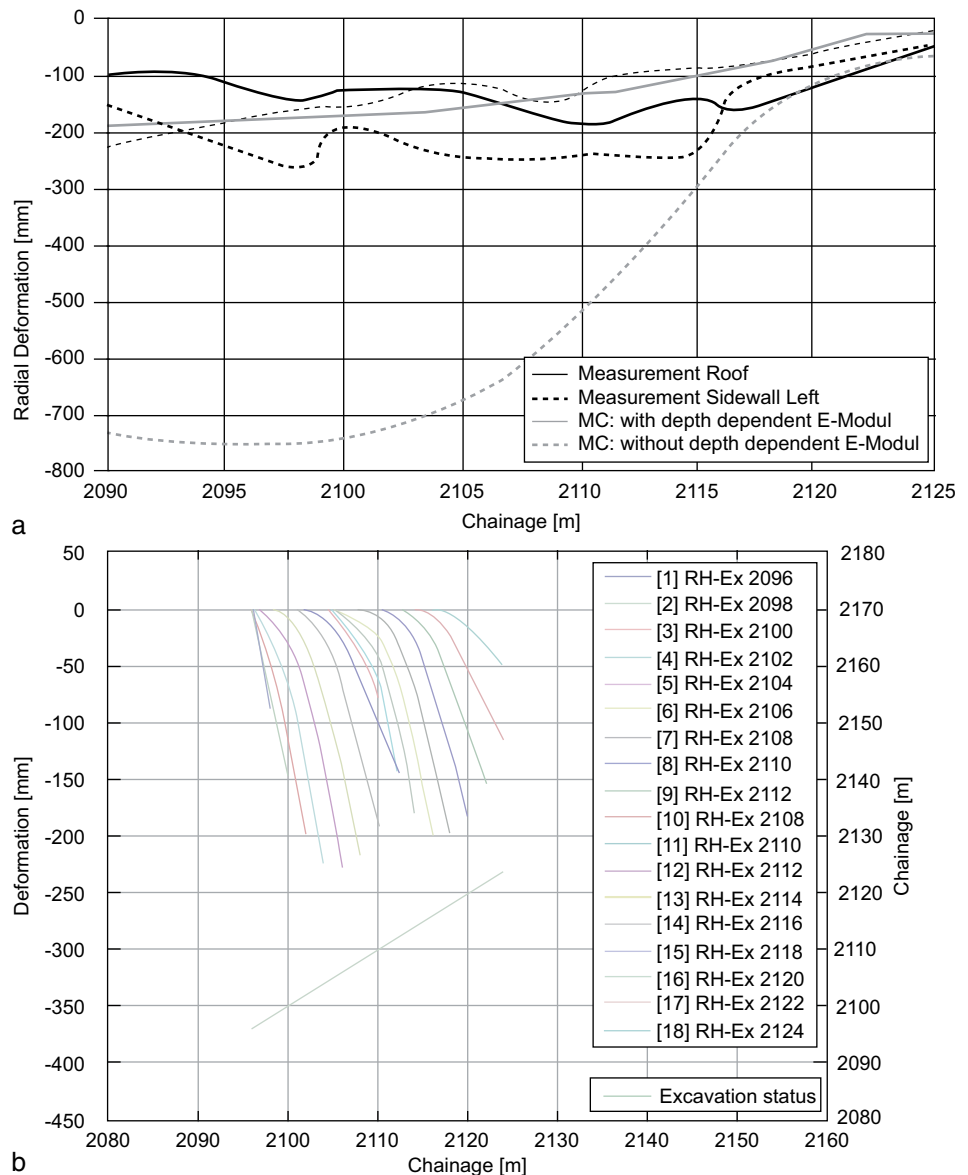
During each excavation round, Young's moduli in front of the face and in radial direction were adjusted (Fig. 4b).

3.4 Implementation of Support Elements

The amount of the implemented support was gathered from the monthly project reports and the design drawings.

Face bolts and rock bolts in radial direction were implemented with a passive cohesion increase as suggested by Egger [8] and Wullschläger [9]. The installation of the steel arches was simulated with beam elements in the numerical model. The beam elements were activated at a distance of 15–20 m behind the face, simulating closing the friction loops on the construction site. The distance of closing the friction loop and installing the steel arches in the numerical simulation was determined by investigating the time-displacement lines of the measurement results for the different cross sections. This distance varied between 15 and 20 m behind the face. The shotcrete was installed at a distance of about 30 m to the face where radial deformations already declined.

Fig. 5: a Measurement results and results from simulation (radial deformations). **b** Core extrusion when using a depth-dependent Young's Modulus (installing the steel arches 15 m behind the face)
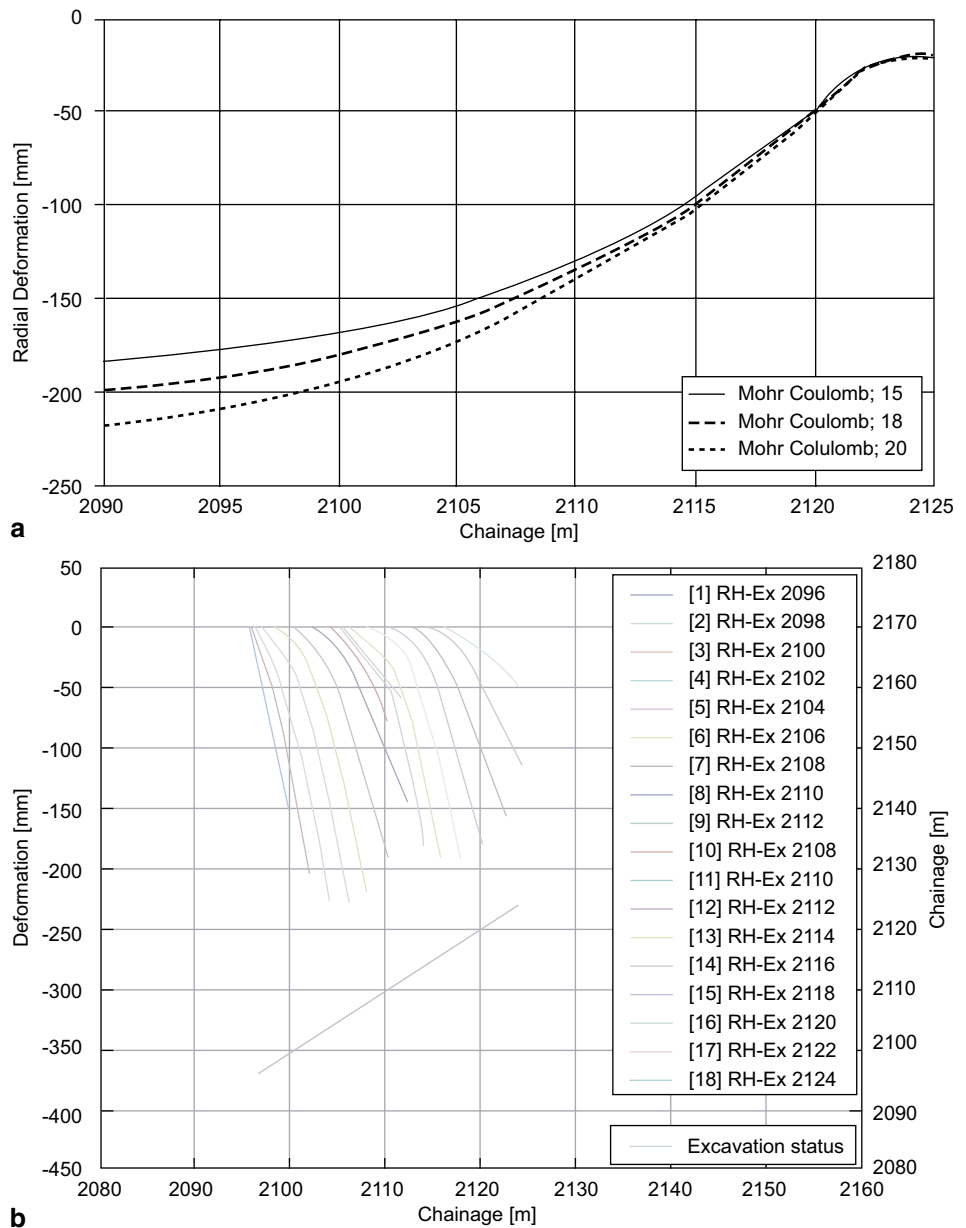

a

b

4. Results and Discussion

4.1 Use of a Depth-dependent Young's Modulus

Figure 5a shows the measured deformations of the tunnel at the crown and the sidewalls. Results at the crown from simulation with and without the use of a depth-dependent Young's modulus when installing the steel arches in a distance of 15 m behind the face are also shown. Figure 5b shows the axial extrusion in front of the face when using a depth-dependent Young's Modulus and installing the steel arches in a distance of 15 m behind the face.

The measurement results for the investigated section show that the deformations vary from 100 to 250 mm at the beginning and the middle of the section and decrease to a value of about 50 mm at the transition to the more competent Aare Massif. The measurable deformations from the numerical simulations without a depth-dependent

Young's modulus vary from about 750 mm at the beginning to about 70 mm at the end of the investigated section. With the implementation of the depth-dependent Young's modulus these deformations decrease to 180 mm at the beginning and 30 mm at the end of the investigated section. Figure 5 shows that deformations are over-predicted by far when using only a homogenous Young's modulus. With the use of a depth-dependent stiffness approach the simulation results meet the measurements from the construction site. The axial extrusion varies between 50 and 230 mm for the different RH-Extensometers. Comparison with the measured core extrusion shows that the simulation results are in good comparison with most of the measurement results from the RH-Extensometers installed at the construction site.

Fig. 6: **a** Simulation results for different steel arches installation distances (radial deformations). **b** Core extrusion when installing the steel arches 20 m behind the face

4.2 Distance of Closing the Friction Loops

With an increasing distance to the face when installing the steel arches, the radial deformations increase as well from 180 mm to 220 mm at the beginning of the investigated section. When entering the more competent Aare Massif the radial deformations for all investigated simulations are similar. Comparison of the core extrusion for different installation distances of the steel arches (Fig. 5b and Fig. 6b) show similar results.
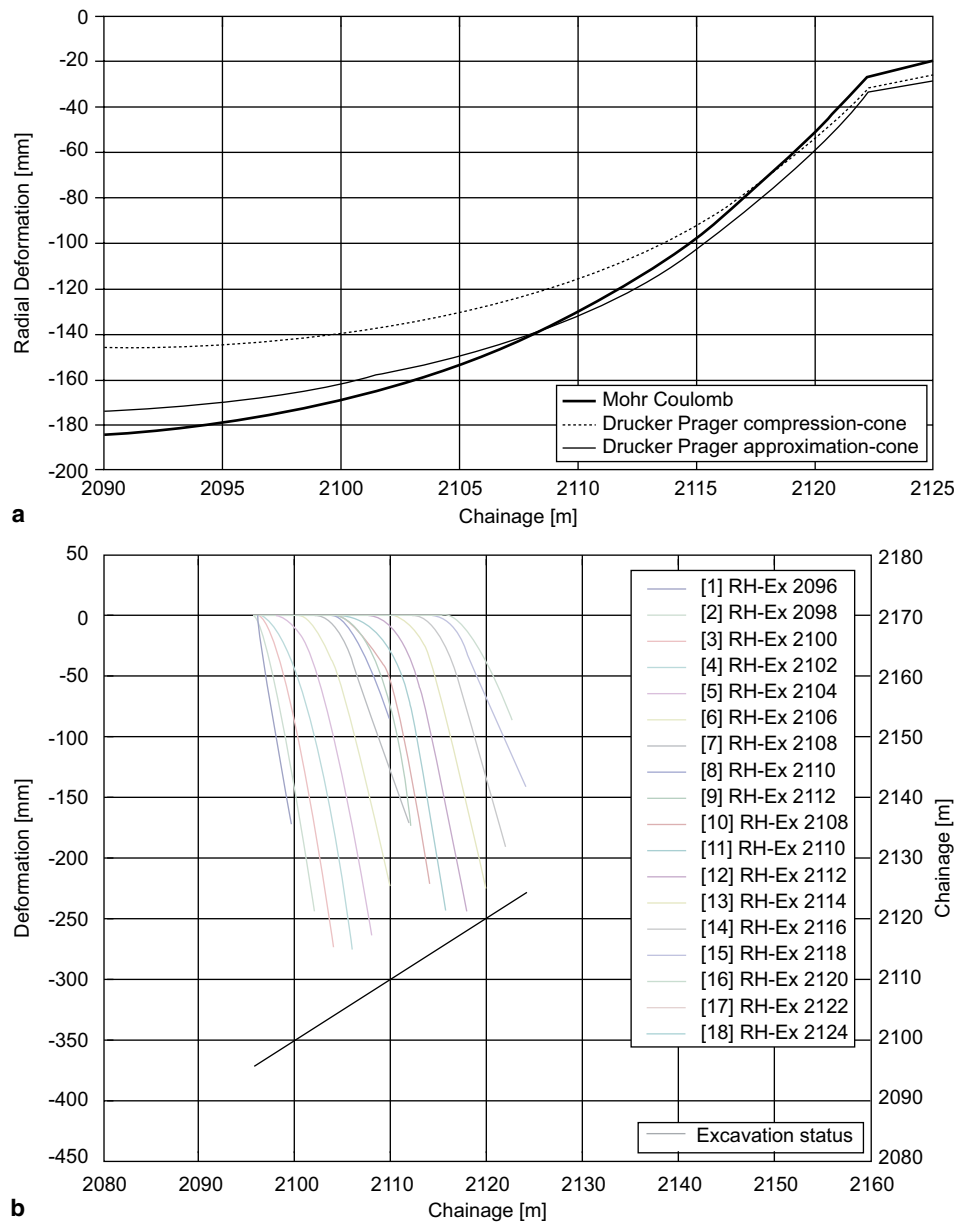
4.3 Different Constitutive Laws

A Mohr Coulomb and a Drucker Prager failure criterion were used. For the simulations using the Drucker Prager failure criterion two parameter sets were used as mentioned in Sect. 3.2. Figure 7a shows the radial deformations when installing the steel arches in a distance of 15 m behind the face for the different constitutive laws used. In Fig. 7b the core extrusions when using the Drucker Prager approximation cone is shown.

With the parameter set for the approximation-cone the simulation results are similar to the ones using the Mohr Coulomb failure criterion. By using the parameters for the compression cone the deformations are smaller. The core extrusions on the other hand are higher than the simulation results using a Mohr Coulomb failure criterion.

In addition, it is interesting to mention Cantieni et al. [10], who investigated the connection between radial displacements and the core extrusion in front of the face for the Gotthard Base Tunnel. It was found that it is only possible to a certain extent to predict radial deformations based on results from RH-Extensometers.

Fig. 7: a Results for simulations with a Mohr Coulomb and a Drucker Prager failure criterion. **b** Core extrusion when using the Drucker Prager approximation cone

5. Conclusion

It has been shown that it is possible to obtain comparable results between numerical simulations and measurement results of such a challenging construction site as the Gotthard Base Tunnel. This is valid when looking into radial displacements and the extrusion of the face.

A prerequisite for these simulations is to have very good geological and geotechnical documentation during the design and the construction stage as was the case during the construction of the Gotthard Base Tunnel. Especially the determination of Young's moduli with different side pressures has great relevance for predicting deformations in tunnels with squeezing conditions.

Furthermore it has been shown that the installation time of the support elements has an influence on the radial displacements, but nearly no influence on the core extrusions in front of the face.

References

1. Kovari, K. (2009). Design Methods with Yielding Support in Squeezing and Swelling Rocks. World Tunnel Congress. Budapest, Hungary.
2. Vogelhuber, M. (2007). Der Einfluss des Porenwasserdrucks auf das mechanische Verhalten kakiritisierter Gesteine. PhD Thesis. ETH Zurich. Zurich, Switzerland.
3. Anagnostou, G., Pimentel, E., Cantieni, L. (2008). Report on behalf of AlpTransit Gotthard Ltd.: Felsmechanische Laborversuche Los 378—Schlussbericht—AlpTransit Gotthard Basistunnel, Teilabschnitt Sedrun. ETH Zurich, Institute for Geotechnical Engineering. Chair of Underground Construction. Zurich, Switzerland.
4. Thut, A., Nateropp, D., Steiner, P., Stolz, M. (2006). Tunnelling in squeezing rock – yielding elements and face control. 8th International Conference on Tunnel Construction and Underground Structures. Ljubljana.
5. Asef, M., Reddish, D.J. (2002). The impact of confining stress on the rock mass deformation modulus, Géotechnique 52, 4, 235–241.
6. Verman, M., Singh, B., Viladkar, N., Jethwa, J.L. (1997). Effect of Tunnel Depth on Modulus of Deformation of Rock Mass. Rock Mech. Rock Eng. 30, 3, 121–127.
7. Sulem, J., Panet, M., Guenot, A. (1987). An Analytical Solution for Time-dependent Displacements in a Circular Tunnel. International Journal of Rock Mechanics and Mining Sciences & Geomechanics Abstracts 24. 155–164.
8. Egger, P. (1973). Einfluss des Post-Failure Verhaltens von Fels auf den Tunnelausbau unter besonderer Berücksichtigung des Ankerausbaus, Universität Karlsruhe, Dissertation.
9. Wullschläger, D. (1988). Ein Verbundwerkstoffmodell für die Systemankerung im Tunnelbau. Dissertation. Universität Karlsruhe.
10. Cantieni, L., Anagnostou, G., Hug, R. (2011). Interpretation of Core Extrusion Measurements When Tunnelling Through Squeezing Ground. Rock Mech. and Rock Eng. 44, 641–670.